Shear Alfvén spectrum in heliotron systems - continuum and point spectra -

NIFS N.Nakajima

Motivation

1. In LHD experiments, energetic particle-driven modes [TAE, GAE, R-TAE(EPM), and HAE] have been observed. The identification is based on the structure of the shear Alfvén spectra and the resonance conditions.
2. On the other hand, the reconstruction of MHD equilibrium is fairly difficult in helical systems (plasma boundary, net toroidal current profile)

Purposes

1. To clarify the structure of the shear Alfvén spectrum in heliotron systems.
2. To use such the information of spectrum for the reconstruction of MHD equilibrium

Contents

TAE : Toroidicity-induced shear Alfvén Eigenmodes
[C.Z.Cheng, L.Chen, and M.S.Chance, Ann.Phys. (NY) **161** 21 (1984)]
HAE : Helicity-induced shear Alfvén Eigenmodes
[N.Nakajima, C.Z.Cheng, and M.Okamoto, Phys.Fluids B **4** 1115 (1992)]

1 Gap frequencies

$$\Omega(\psi) = \frac{\omega}{\omega_A(\psi)}, \quad \omega_A(\psi): \quad \text{local Alfvén frequency}$$

in double symmetric systems
[straight tokamak with circular cross section]

$$\Omega(\psi) = |m - nq(\psi)| \ : \ \text{continuum}$$

in general tori

$$\Omega(\psi) = |m - nq(\psi)|, \quad \Omega' = |m' - n'q(\psi)|$$

$$\left\{ \begin{array}{l} \Omega(\psi) = \Omega'(\psi) \\ m' = m + m_{eq}, \quad n' = n + n_{eq} \end{array} \right\}$$

$$\Downarrow$$

$$\Omega(\psi) \ = \ \frac{1}{2}|m_{eq} - n_{eq}q(\psi)|, \quad q(\psi) \ = \ \frac{2m + m_{eq}}{2n + n_{eq}}$$

A) Symmetric systems

1) axisymmetric tori

$$n_{eq} = 0, \quad \Omega(\psi) = \frac{1}{2}|m_{eq}|, \quad q(\psi) = \frac{2m + m_{eq}}{2n}$$

$$\begin{array}{llcll} m_{eq} = 1 & \text{(toroidicity)} & \rightarrow & \Omega = \frac{1}{2} & : \text{TAE gap} \\ m_{eq} = 2 & \text{(ellipticity)} & \rightarrow & \Omega = 1 & : \text{EAE gap} \\ m_{eq} = 3 & \text{(triangularity)} & \rightarrow & \Omega = \frac{3}{2} & : \text{NAE gap} \end{array}$$

2) straight helical systems

$$m_{eq} = kM, n_{eq} = kN, \quad \Omega(\psi) = \frac{1}{2}k|M - Nq(\psi)|, \quad q(\psi) = \frac{2m + kM}{2n + kN}$$

$$k = 1, 2, \cdots \; : \; \text{HAE gap}$$

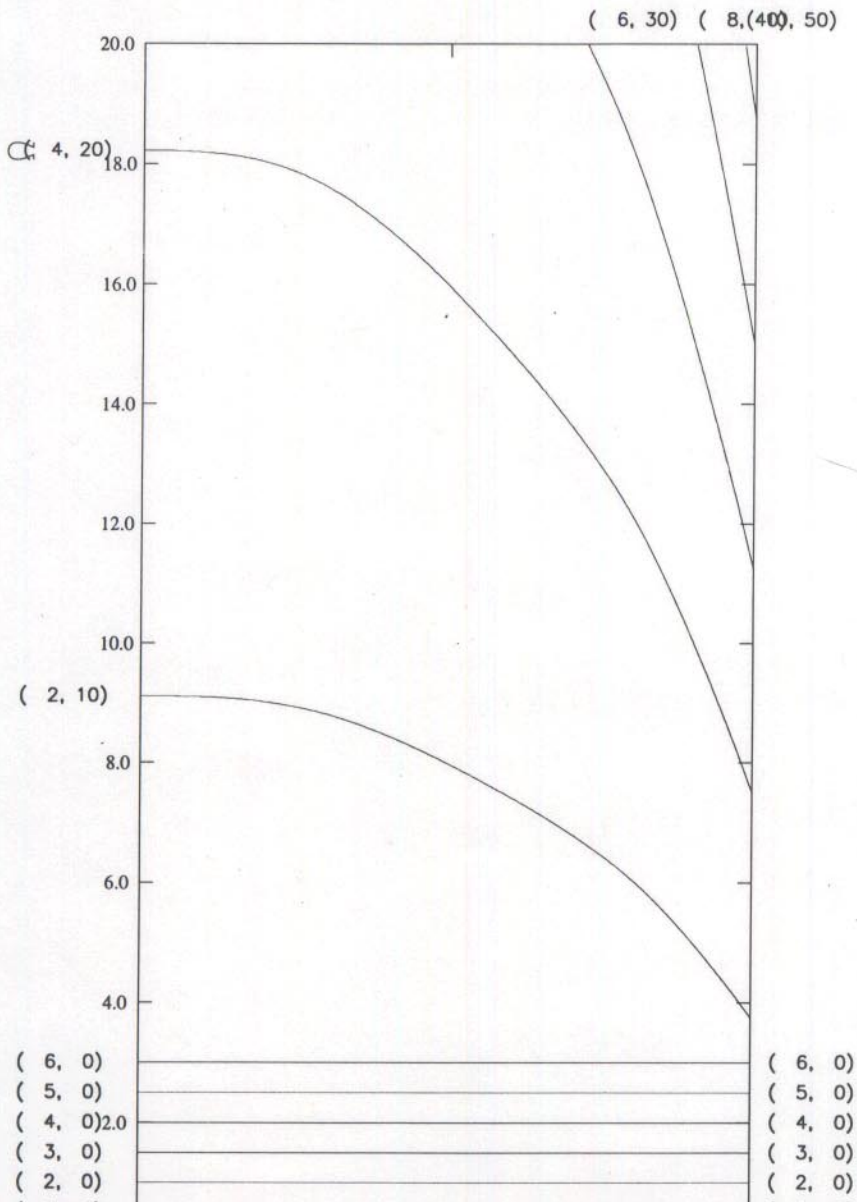

(6, 30) (8,(40), 50)
20.0
℄(4, 20)
18.0
16.0
14.0
12.0
10.0
(2, 10)
8.0
6.0
4.0
(6, 0)
(5, 0)
(4, 0)
2.0
(3, 0)
(2, 0)
(1, 0)
(6, 0)
(5, 0)
(4, 0)
(3, 0)
(2, 0)
(1, 0)

B) Asymmetric tori with N field period
($N = 10$ for LHD)

$$n_{eq} = kN, \quad \Omega(\psi) = \frac{1}{2}|m_{eq} - kNq(\psi)|, \quad q(\psi) = \frac{2m + m_{eq}}{2n + kN}, \quad k = 0, \pm 1,$$

combination of TAE, EAE, NAE, $\cdots$, and various HAE gaps

$$\Downarrow$$

The width of spectral gaps in the range of HAE frequency becomes narrow.

Mode family

Mode families of perturbations are created by the field period:

$$\text{Num.} = \left[\frac{N}{2}\right] + 1, \quad (= 6 \text{ for LHD})$$

For perturbation with $n \geq 0$,

$$\begin{aligned} N_f &= 1, \quad n = 1, 9, 11, 19, \cdots \\ N_f &= 2, \quad n = 2, 8, 12, 18, \cdots \\ N_f &= 3, \quad n = 3, 7, 13, 17, \cdots \end{aligned}$$

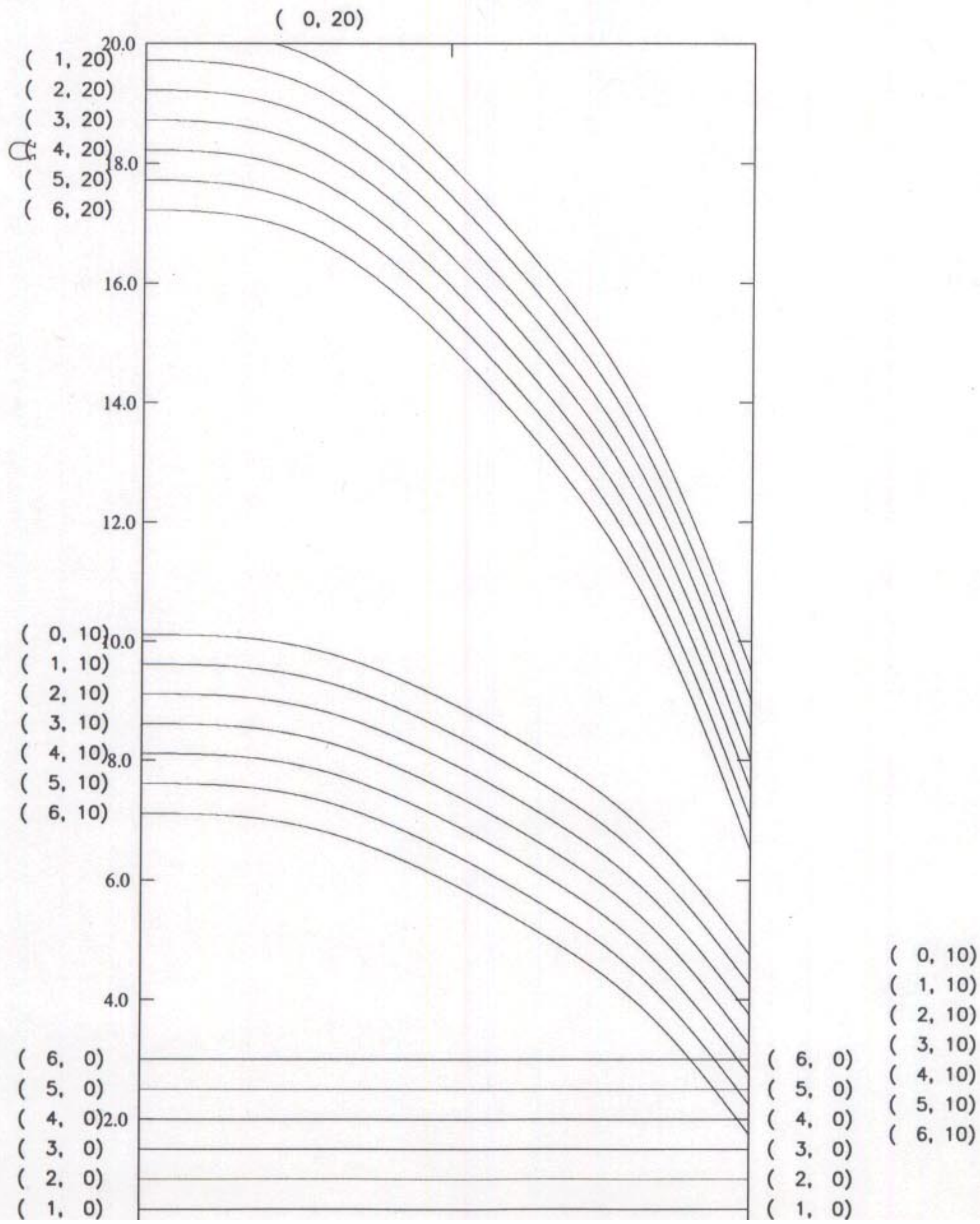

(0, 20)
(1, 20)
(2, 20)
(3, 20)
(4, 20)
(5, 20)
(6, 20)
20.0
18.0
16.0
14.0
12.0
10.0
8.0
6.0
4.0
2.0
(0, 10)
(1, 10)
(2, 10)
(3, 10)
(4, 10)
(5, 10)
(6, 10)
(6, 0)
(5, 0)
(4, 0)
(3, 0)
(2, 0)
(1, 0)

2 Discrete modes (Point spectra)

A) Symmetric systems

high-n modes in the field line coordinates (ψ, η, α)

$$\frac{d^2\xi}{d\eta^2} + \left[\underbrace{a - 2\varepsilon\cos(2\eta)}_{\text{Mathieu}} - F(\eta) \right] \xi = 0$$

where

for high-n TAE

$$\begin{aligned}
\eta &= \frac{\theta}{2}, \quad a \;=\; (2\Omega)^2, \\
\varepsilon &= -2a\varepsilon_t \;\Leftarrow\; \text{toroidicity}, \\
F(\eta) &= \frac{(2s)^2}{[1+(2s\eta)^2]^2} \;:\; \text{local potential}
\end{aligned}$$

for high-n HAE

$$\begin{aligned}
\eta &= (m_{eq} - n_{eq}q)\frac{\theta}{2}, \quad a \;=\; \left[\frac{2\Omega}{m_{eq} - n_{eq}q}\right]^2, \\
\varepsilon &= 2\frac{d^2\varepsilon_h}{d\rho^2} - (a+1)\varepsilon_h \Leftarrow \text{ ellipticity or triangularity}, \\
F(\eta) &= \frac{[2(m_{eq} - n_{eq}q)s]^2}{[(m_{eq} - n_{eq}q)^2 + (2s\eta)^2]^2} + \cdots \;:\; \text{local potential}
\end{aligned}$$

unstable region of Mathieu $\Rightarrow$ spectral gaps
stable region of Mathieu $\Rightarrow$ continuum

Local potential $F(\eta)$ makes point spectra in the spectral gaps.

B) Asymmetric tori

$$\frac{d^2\xi}{d\eta^2} + \left[\underbrace{a - 2\varepsilon\cos(2\eta)}_{\text{Mathieu}} - F(\eta)\right]\xi = 0,$$

$$F(\eta) = 2\varepsilon'\cos(2\lambda\eta), \quad \lambda: \text{ irrational number}$$

When $|\varepsilon|$ and $|\varepsilon'|$ become large and same order, the potential becomes quasi-periodic, leading to the existence of Point spectra (asymmetric modes).

Note

1. **Point spectra are created by a non-periodic (local or non-local) perturbation superposed on a periodic potential.**

2. To create point spectra (TAE, HAE, and so on) in the symmetric systems, the magnetic shear (s) is needed.

3. To create point spectra (asymmetric modes), a quasi-periodic potential (irrational λ) is needed.

3 Shear Alfvén spectra of LHD

shear Alfvén branch

$$\vec{B}\cdot\nabla\left[\frac{|\nabla\psi|^2}{B^2}\vec{B}\cdot\nabla\hat{\xi}\right]+\omega^2\rho_m\frac{|\nabla\psi|^2}{B^2}\hat{\xi}=0$$

In Boozer coordinates (ψ,θ,ζ),

$$\begin{aligned}
L\hat{\xi} &\equiv \left(\frac{\partial}{\partial\theta}+q\frac{\partial}{\partial\zeta}\right)\left[|\nabla\psi|^2\left(\frac{\partial}{\partial\theta}+q\frac{\partial}{\partial\zeta}\right)\hat{\xi}\right]+\Omega^2|\nabla\psi|^2\left(\frac{\langle B^2\rangle}{B^2}\right)^2\hat{\xi}\\
&= 0,\\
\Omega^2 &= \omega^2\tau_A^2,\quad \tau_A^2\equiv\frac{\rho_m}{\left(2\pi\iota\!\!\text{-}\frac{d\Phi_T}{dV}\right)^2}
\end{aligned}$$

Note only two quantities $|\nabla\psi|^2$ and $|\nabla\psi|^2\left(\frac{\langle B^2\rangle}{B^2}\right)^2$ determine the shear Alfvén spectrum.

$$|\nabla\psi| \;\Rightarrow\; \text{change in shape}$$

$$\frac{\langle B^2\rangle}{B^2} \;\Rightarrow\; \text{change in field strength}$$

Note in helical systems, plasma shaping may significantly affect the shear Alfvén spectrum.

A) Lagrangian approach (by self-adjointness)

$$
\begin{aligned}
\mathcal{L} &\equiv \int d\theta \int d\zeta \hat{\xi} L \hat{\xi} \\
&= \int d\theta \int d\zeta \left[\Omega^2 |\nabla\psi|^2 \left(\frac{\langle B^2 \rangle}{B^2} \right)^2 \hat{\xi}^2 - |\nabla\psi|^2 \left(\frac{\partial \hat{\xi}}{\partial \theta} + q \frac{\partial \hat{\xi}}{\partial \zeta} \right)^2 \right]
\end{aligned}
$$

Let $\hat{\xi} = \sum_i a_i \cos(m_i\theta + n_i\zeta)$, then

$$
\mathcal{L} = \vec{X}^T M \vec{X}, \quad \vec{X}^T = (a_1, a_2, \cdots, a_I),
$$

$$
\begin{aligned}
M_{ij} &= \int d\theta \int d\zeta \left[\Omega^2 |\nabla\psi|^2 \left(\frac{\langle B^2 \rangle}{B^2} \right)^2 \cos(m_i\theta + n_i\zeta) \cos(m_j\theta + n_j\zeta) \right. \\
&- \left. |\nabla\psi|^2 (m_i + qn_i)(m_j + qn_j) \sin(m_i\theta + n_i\zeta) \sin(m_j\theta + n_j\zeta) \right]
\end{aligned}
$$

$$
\begin{aligned}
\delta\mathcal{L} = 0 \;&\Rightarrow\; M\vec{X} = 0, \\
\det M = 0 \;&\Rightarrow\; \text{eigenvalues}: \;\; \Omega^2 = \Omega^2(\psi)
\end{aligned}
$$

- advantage
  1. Whole structure of shear Alfvén spectrum is easily seen.
  2. By selecting Fourier modes of equilibrium and perturbation, we can see which modes are related to the spectrum considered.
- disadvantage
  1. It is difficult to distinguish between continua and point spectra.

N1m676−sel−M1(L=all,M=0,10,20): Ω is normalized at each flux surface Input modes: 676

Input modes are not sorted.: iss = 1: ise = 1001: nsdnew = 1001

NFP = 10: Ω_{min} = 0.000D+00: Ω_{max} = 2.000D+01: δΩ = 1.000D−02

NBZMIN = −10: NBZMAX = 10: MBZMAX = 60: NSD = 61

NLC = 128: NLP = 16: INPM = 676: cos phase used.

MEQMOD = 60: NEQMOD = 6: N ≧ 0

(0, 1)		(11, 9)		(
(1, 1)		(12, 9)		(
(2, 1)		(13, 9)		(
(3, 1)		(14, 9)		(
(4, 1)		(15, 9)		(
(5, 1)		(16, 9)		(
(6, 1)		(17, 9)		(
(7, 1)		(18, 9)		(
(8, 1)		(19, 9)		(1
(9, 1)		(20, 9)		(1
(10, 1)		(21, 9)		(1
(11, 1)		(22, 9)		(1
(12, 1)		(23, 9)		(1
(13, 1)		(24, 9)		(1
(14, 1)		(25, 9)		(1
(15, 1)		(26, 9)		(1
(16, 1)		(27, 9)		(1
(17, 1)		(28, 9)		(1
(18, 1)		(29, 9)		(2
(19, 1)		(30, 9)		(2
(20, 1)		(31, 9)		(2
(21, 1)		(32, 9)		(2
(22, 1)		(33, 9)		(2
(23, 1)	O	(34, 9)		(2
(24, 1)	O	(35, 9)		(2
(25, 1)	O	(36, 9)		(2
(26, 1)	O	(37, 9)		(2
(27, 1)	O	(38, 9)		(2
(28, 1)	O	(39, 9)	O	(3
(29, 1)	O	(40, 9)	O	(3
(30, 1)	O	(41, 9)	O	(3
(31, 1)	O	(42, 9)	O	(3
(32, 1)	O	(43, 9)	O	(3
(33, 1)	O	(44, 9)	O	(3
(34, 1)	O	(45, 9)	O	(3
(35, 1)	O	(46, 9)	O	(3
(36, 1)	O	(47, 9)	O	(3
(37, 1)	O	(48, 9)	O	(3
(38, 1)	O	(49, 9)	O	(4
(39, 1)	O	(50, 9)	O	(4
(−1, 1)		(51, 9)	O	(4
(−2, 1)		(52, 9)	O	(4
(−3, 1)		(53, 9)	O	(4
(−4, 1)		(54, 9)	O	(4
(−5, 1)		(55, 9)	O	(4
(−6, 1)		(56, 9)	O	(4
(−7, 1)		(57, 9)	O	(4
(−8, 1)		(58, 9)	O	(4
(−9, 1)		(59, 9)	O	(5
(−10, 1)		(60, 9)	O	(5
(−11, 1)		(61, 9)	O	(5
(−12, 1)		(62, 9)	O	(5
(−13, 1)		(63, 9)	O	(5
(−14, 1)		(64, 9)	O	(5
(−15, 1)		(65, 9)	O	(5
(−16, 1)		(66, 9)	O	(5
(−17, 1)		(67, 9)	O	(5
(−18, 1)		(68, 9)	O	(5
(−19, 1)		(69, 9)	O	(6
(−20, 1)	O	(−1, 9)		(6
(−21, 1)	O	(−2, 9)		(6
(−22, 1)	O	(−3, 9)		(6
(−23, 1)	O	(−4, 9)		(6
(−24, 1)	O	(−5, 9)		(6
(−25, 1)	O	(−6, 9)		(6
(−26, 1)	O	(−7, 9)		(6
(−27, 1)	O	(−8, 9)		(6
(−28, 1)	O	(−9, 9)		(6
(−29, 1)	O	(−10, 9)		(7
(0, 9)		(−11, 9)	O	(7
(1, 9)		(−12, 9)	O	(7
(2, 9)		(−13, 9)	O	(7
(3, 9)		(−14, 9)	O	(7
(4, 9)		(−15, 9)	O	(7

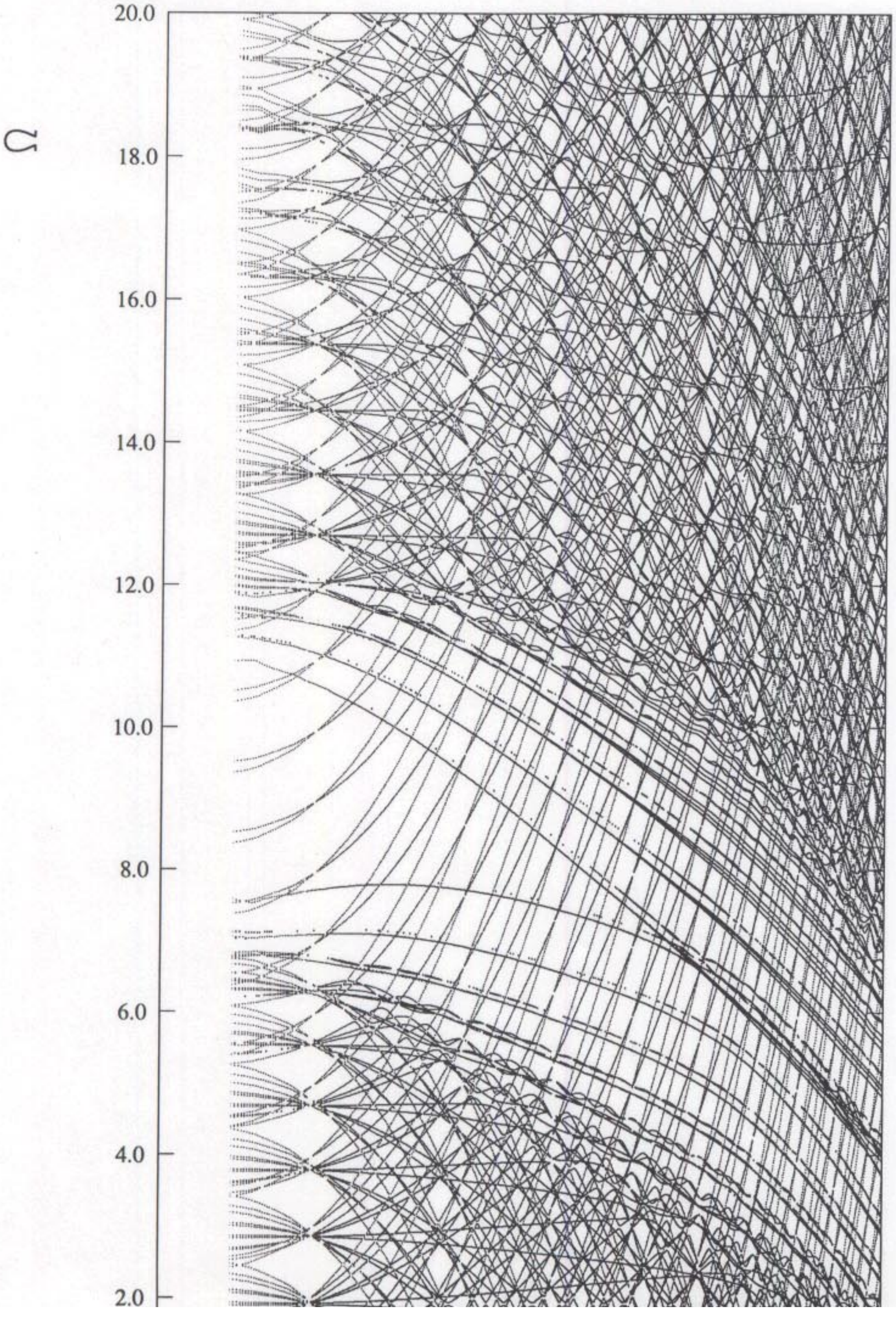

Note in the case of LHD,

1. The spectral gap is so complicated that a large number of Fourier modes of equilibrium and perturbations are needed.

2. When a large number of Fourier modes are used, the shear Alfvén spectra between different mode families are almost same (there is no essential differences between mode families).

3. The shape of the plasma cross section significantly affects the structure of the HAE spectral gap.

   (a) The ellipticity expressed by $(m_{eq}, n_{eq}) = (2, 10)$ makes a large spectral gap in a whole plasma region.

   (b) Other Fourier components around $m_{eq} = 2$ have a same order of amplitude, thus shear Alfvén continua between spectral gaps around $\Omega = |m_{eq} - qn_{eq}|/2 \;\; [(m_{eq}, n_{eq}) = (2, 10)]$ become quite thin.

   (c) Moreover, the merging of the thin Alfvén continua occurs, which may lead to the split of the thin continua in the plasma periphery.

   (d) It is not so clear which spectrum is continuum.

B) Boundary value approach

By changing the coordinates from (ψ, θ, ζ) to (ψ, η, α),

$$\eta = \theta \; (-\infty < \eta < +\infty), \quad \alpha = \zeta - q\theta,$$

self-adjoint type equation:

$$\begin{aligned} L\hat{\xi} &= \frac{\partial}{\partial \eta}\left[|\nabla\psi|^2 \frac{\partial}{\partial \eta}\hat{\xi}\right] + \Omega^2 |\nabla\psi|^2 \left(\frac{\langle B^2 \rangle}{B^2}\right)^2 \hat{\xi} = 0, \\ \Omega &= \Omega(\psi, \alpha) \end{aligned}$$

Boundary condition:

$$\hat{\xi}(\eta = \pm L) = 0$$

1. Fourier modes of the MHD equilibrium can be selected before the coordinate transformation.
2. All of Fourier modes of the perturbation are included (all mode families are combined).

Comparison with high-n ballooning equation

Through $\xi = |\nabla\psi|\hat{\xi}$,

Schrödinger type of equation of shear Alfven modes:

$$
\begin{aligned}
L\xi &= \frac{\partial^2 \xi}{\partial \eta^2} + \left[\Omega^2 \left(\frac{\langle B^2 \rangle}{B^2}\right)^2 - U_{SA}(\eta)\right]\xi = 0, \\
\Omega &= \Omega(\psi, \alpha) \\
U_{SA}(\eta) &= \frac{1}{|\nabla\psi|}\frac{\partial^2 |\nabla\psi|}{\partial \eta^2}
\end{aligned}
$$

Schrödinger type of high-n ballooning equation

$$
\begin{aligned}
L\xi &= \frac{\partial^2 \xi}{\partial \eta^2} + \left[\Omega^2 \left(\frac{\langle B^2 \rangle}{B^2}\right)^2 - U_{high}(\eta)\right]\xi = 0, \\
\Omega &= \Omega(\psi, \theta_k, \alpha) \\
U_{high}(\eta) &= \frac{1}{|\vec{k}_\perp|}\frac{\partial^2 |\vec{k}_\perp|}{\partial \eta^2} - \frac{2}{B^2 |\vec{k}_\perp|^2}\vec{B} \times \vec{\kappa} \cdot \vec{k}_\perp \vec{B} \times \nabla P \cdot \vec{k}_\perp
\end{aligned}
$$

Note

$$
\lim_{\eta \to \infty} U_{high}(\eta) = U_{SA}(\eta)
$$

The solutions of shear Alfvén equation correspond to such solutions of high-n ballooning equation that are not influenced by the local potential due to the magnetic shear and magnetic curvature.

Ω (odd) : 6.69175D−01

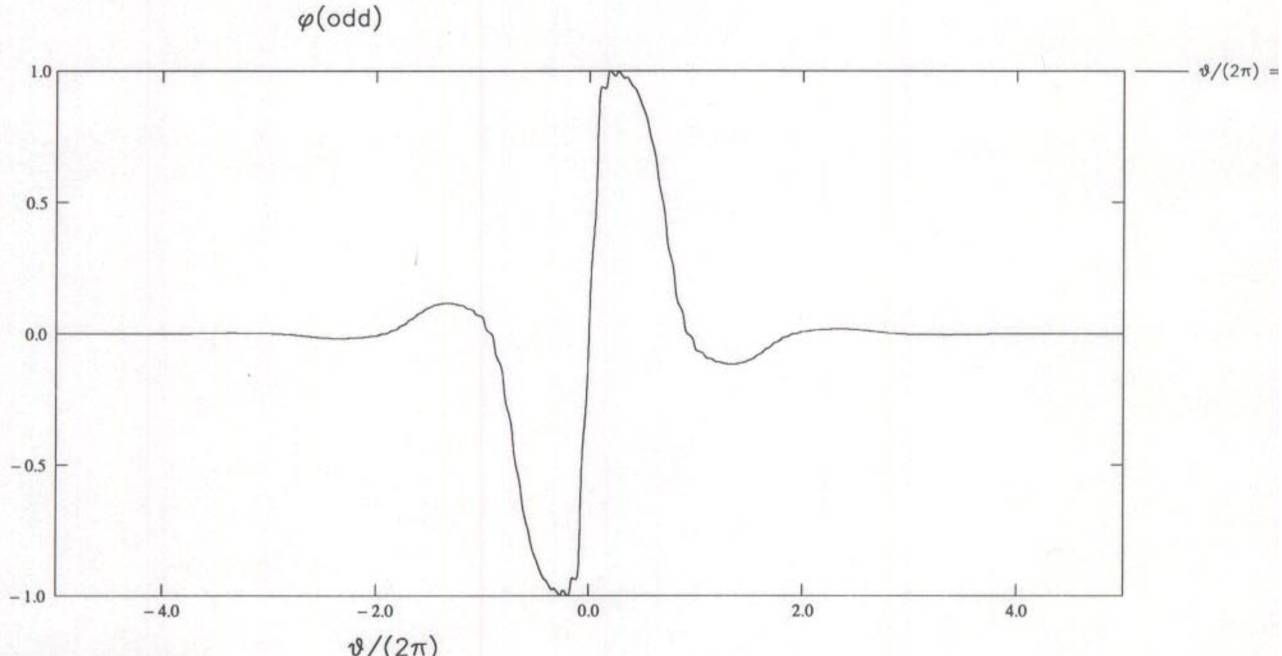

Ω(even) : 7.66555D−01

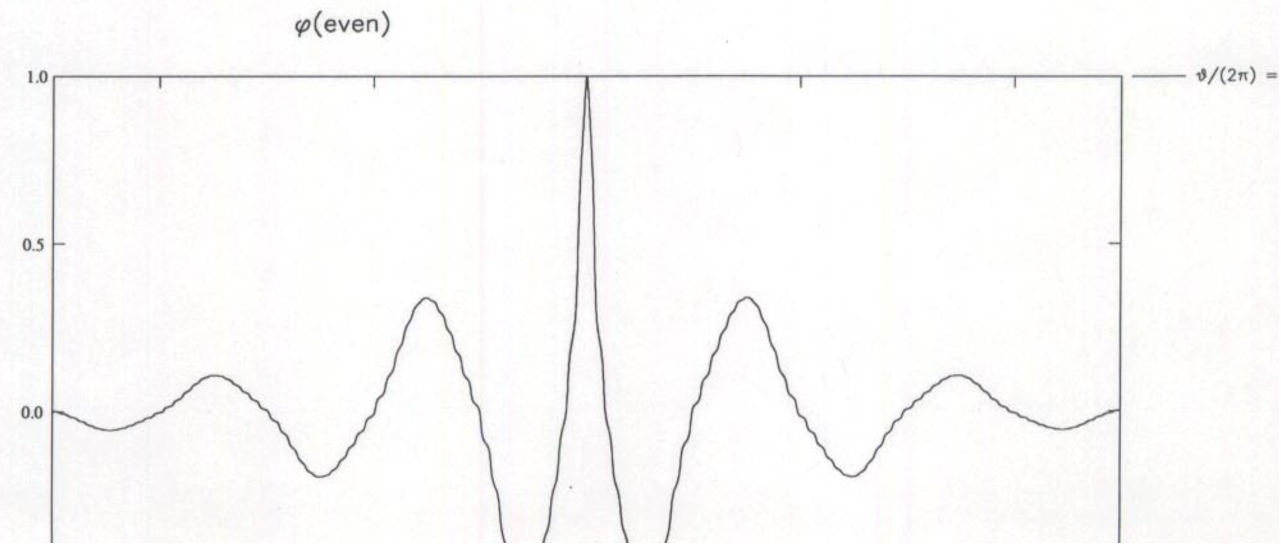

Ω (odd) : 3.67601D+00

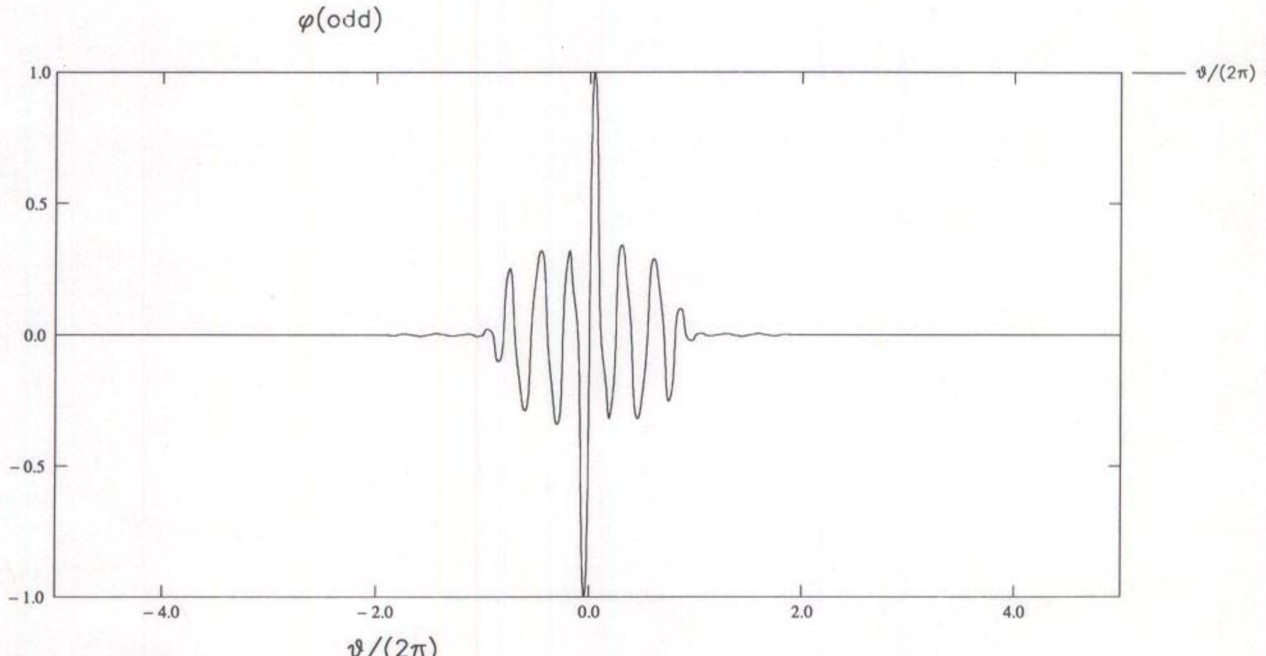

Ω(even) : 3.76006D+00

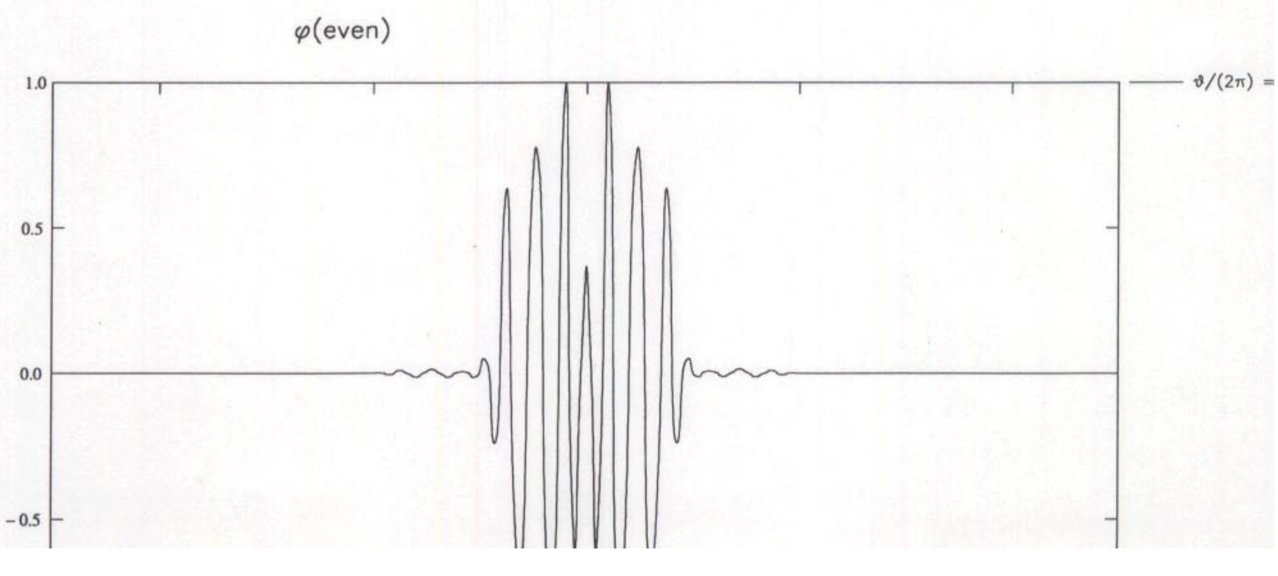

C) Leapunov exponent and winfing number

$$\text{phase} \quad : \quad \tan\phi \equiv \frac{\xi}{\dot{\xi}}$$

$$\text{amplitude} \quad : \quad A \equiv \sqrt{\xi^2 + \dot{\xi}^2}$$

Equation of the phase

$$\frac{d\phi}{d\eta} = \frac{1+V(\eta)}{2} + \frac{1-V(\eta)}{2}\cos(2\phi)$$

Linearized eq. of the phase ($\phi \to \phi + \delta\phi$)

$$\frac{d\ln\delta\phi}{d\eta} = -[1-V(\eta)]\sin(2\phi)$$

Note $\quad \delta\phi A^2 = const.$

where

$$V(\eta) \equiv \Omega^2 \left(\frac{\langle B^2 \rangle}{B^2}\right)^2 - U(\eta),$$

Leapunov exponent : $\Lambda_\phi(\Omega) \equiv \lim_{\eta\to\infty} \dfrac{\ln\delta\phi(\eta) - \ln\delta\phi(\eta_0)}{\eta}$

winding number : $w(\Omega) \equiv \lim_{\eta\to\infty} \dfrac{\phi(\eta)}{\eta}$

Note w is a continuous non-decreasing function of Ω with plateaus (like a devil's staircase).

Classification of eigenvalues

For extended solutions

$$\begin{aligned} \Lambda_\phi &= 0, \ \ (|A| < \infty \Rightarrow |\delta\phi| < \infty) \\ \frac{dw}{d\Omega} &> 0, \ \ (\textbf{continua}) \end{aligned}$$

For localized solutions

$$\begin{aligned} \Lambda_\phi &< 0, \ \ (|A| \to \infty(\text{due to round off error}) \Rightarrow |\delta\phi| \to 0) \\ \frac{dw}{d\Omega} &> 0, \ \ (\textbf{point spectra}) \end{aligned}$$

For diverging solutions

$$\begin{aligned} \Lambda_\phi &< 0, \ \ (|A| \to \infty \Rightarrow |\delta\phi| \to 0) \\ \frac{dw}{d\Omega} &= 0, \ \ (\textbf{gaps}) \end{aligned}$$

Dispersion (even): $\varphi'(0) = 0$

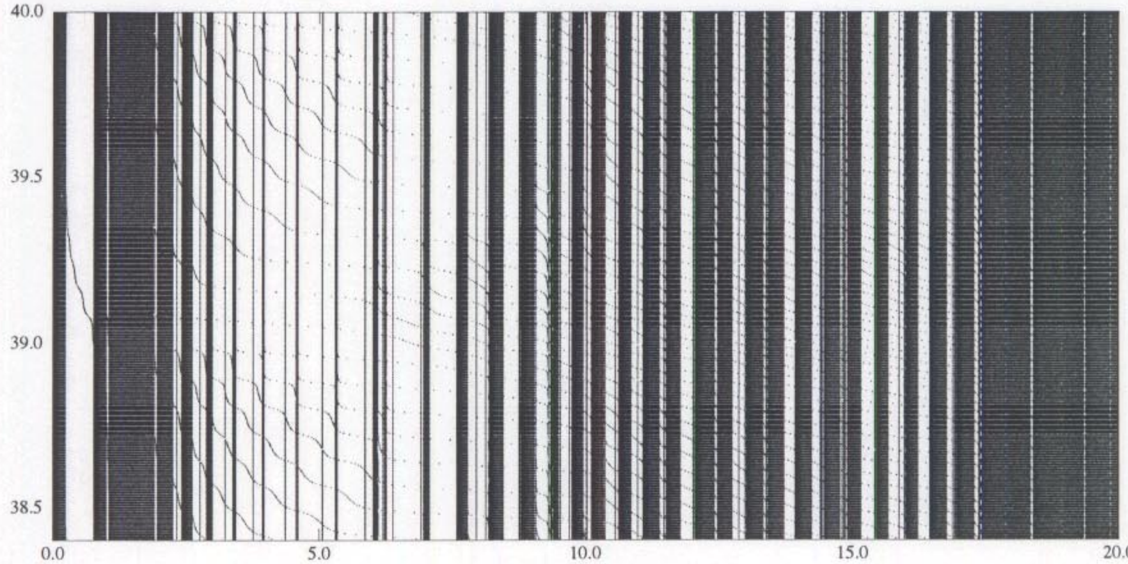

(even): $\varphi'(0)=0$: Winding number

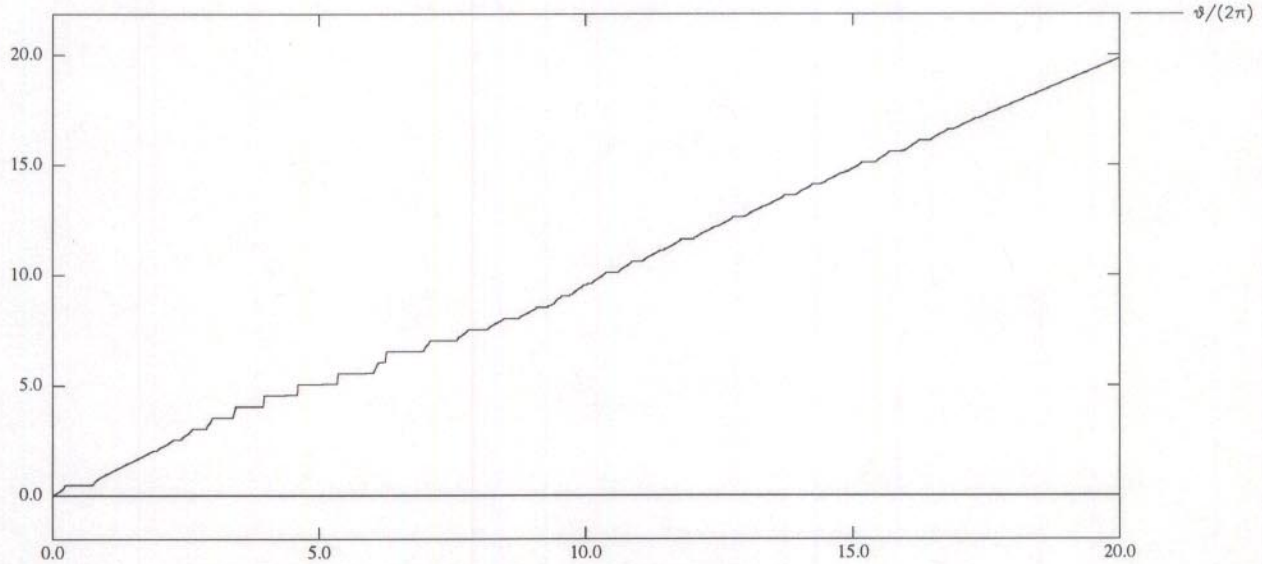

(even): $\varphi'(0)=0$: Lyapunov exponent

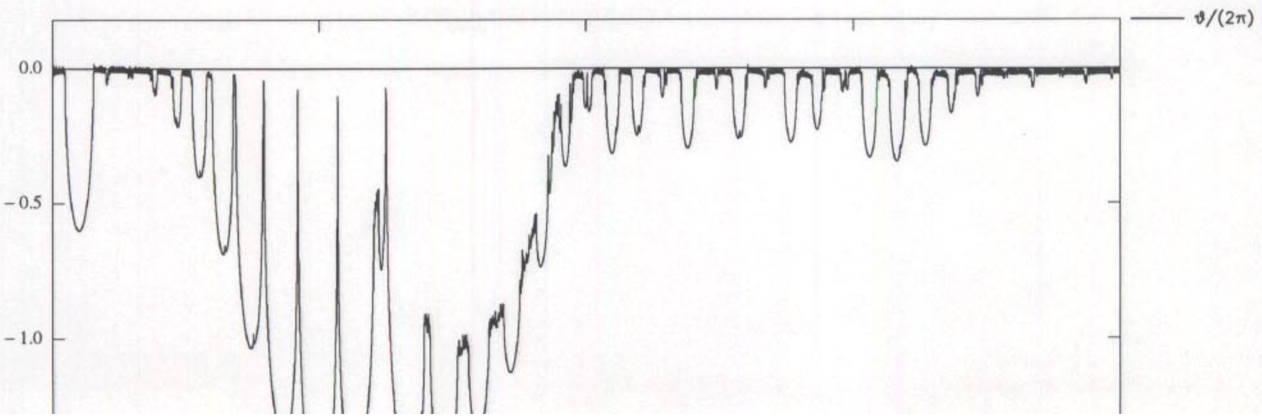

Ω (odd) : 6.01881D+00

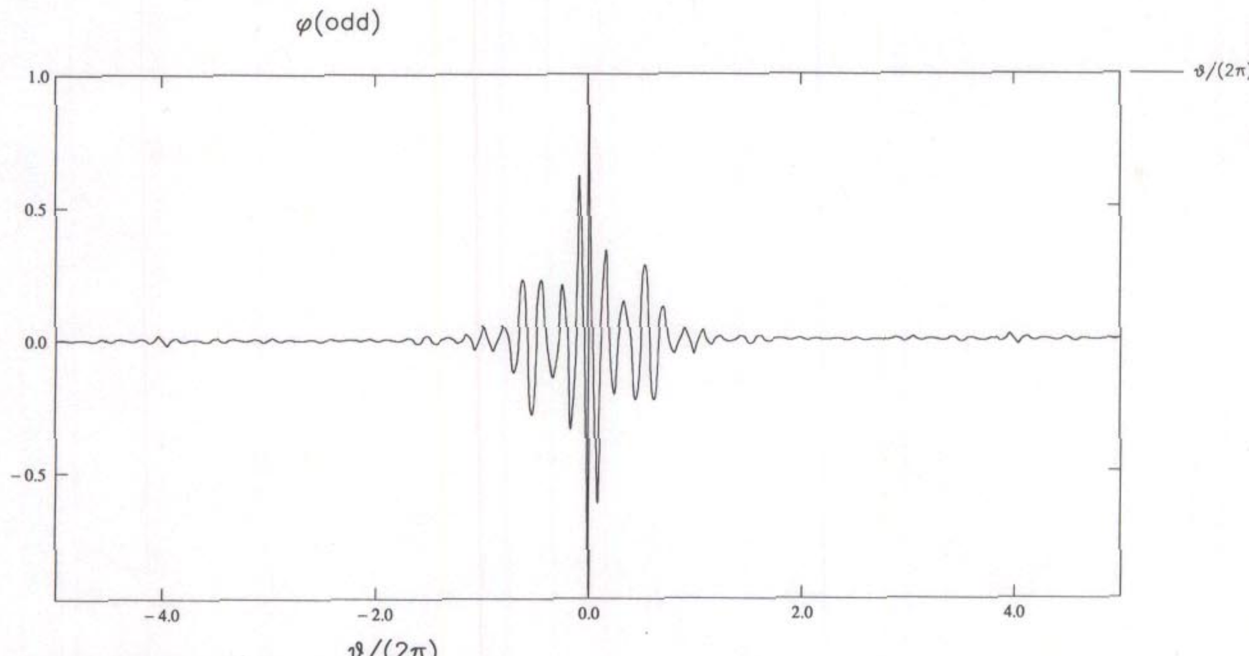

Ω(even) : 6.01881D+00

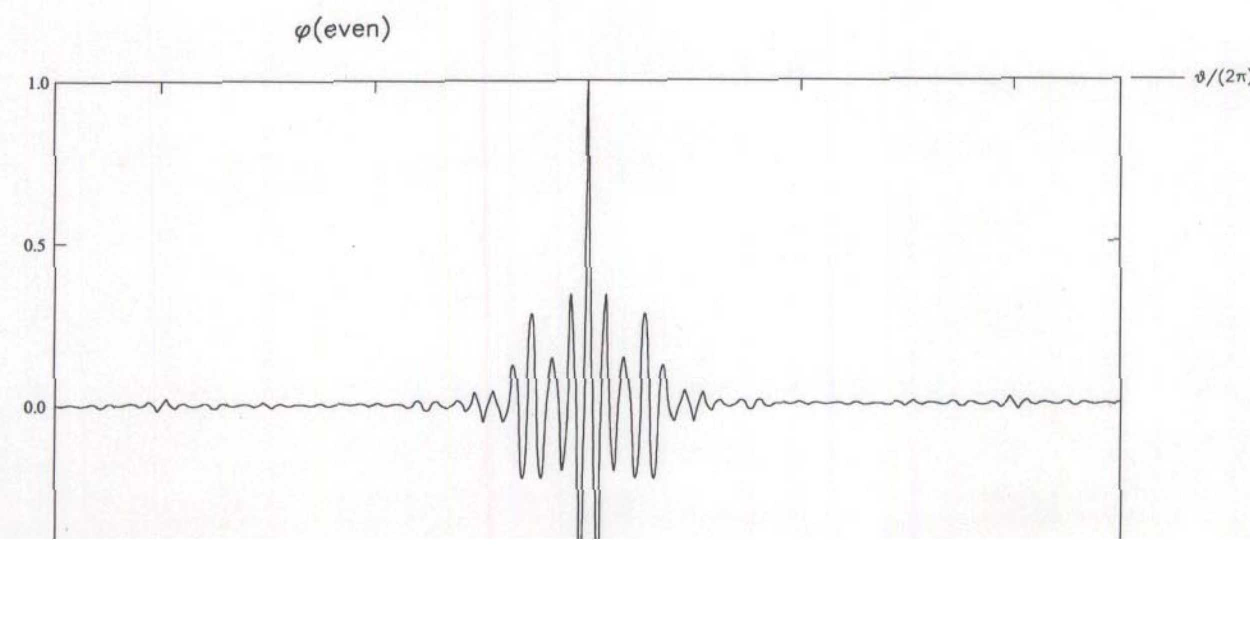

4 Summary of calculations

1. Strong plasma shape deformation makes shear Alfvén continua in HAE frequency range quite thin.
2. Moreover, the merging of such quite thin continua changes the spectral property from the continua into point spectra (asymmetric discrete modes).
   (a) Those point spectra are degenerate: $\Omega_{even} = \Omega_{odd}$.
   (b) Those point spectra are independent of the magnetic field line: $\Omega = \Omega(\psi)$.
   (c) Their radial structure may be like a δ-function.
3. Asymmetric discrete modes exist in the upper half of the HAE frequency range.
4. In the lower half of the HAE frequency range, high-n HAE modes exist between quite thin shear Alfvén continua.
   (a) High-n HAE modes have week (strong) α (θ_k)-dependence: $\Omega \simeq \Omega(\psi, \theta_k)$.
   (b) The global HAE mode may be fairly localized near the plasma edge.
   (c) Expected mode numbers of the global HAE mode for $(m_{eq}, n_{eq}) = (2, 10)$ and $q = 1$ are

$$
\begin{aligned}
(m,n) = \;& (5,1) + (7,11) \\
& (-3,1) + (5,9) \\
\\
& (6,2) + (8,12) \\
& (-2,2) + (4,8)
\end{aligned}
$$

5 Discussions

1. Experimentally observed modes with $f \sim 200$ kHz may be identified as radially localized HAE modes, if the plasma boundary and the density profile are adequately determined.

2. R-TAE or EPM modes with $(m, n) = (2, 1)$ may be excited in LHD, when the rational surface with $\iota = 1/2$ exists in the low shear region near the magnetic axis.

3.

$$\begin{bmatrix} \text{Observation of} \\ \text{TAE, HAE, R-TAE} \end{bmatrix} + \begin{bmatrix} \text{Theoretical} \\ \text{prediction} \end{bmatrix}$$

$$\Downarrow$$

$$[\ \text{more exact reconstruction of MHD equilibrium}\ ]$$